EFFECTS OF SIZE, SPECIES, AND ADJACENT LAMINA ON MOISTURE-RELATED STRAIN IN GLULAM

So Sun Lee
Research Assistant
E-mail: ddgod2865@naver.com

Sung-Jun Pang
Research Professor
E-mail: sjp@jnu.ac.kr

*Gi Young Jeong**†
Associate Professor
Department of Wood Science and Engineering
Chonnam National University
77 Yongbongro Bukgu
Gwangju 500-757, South Korea
E-mail: gjeong1@jnu.ac.kr

(Received September 2017)

Abstract. The goal of this study was to investigate the effects of size and species on moisture-related strain in glued–laminated timber (glulam). Swelling and shrinkage behaviors of different sizes (120 × 120, 180 × 180, and 180 × 240 mm^2) of glulam made from larch and pine were measured using digital image correlation. A new approach to predict dimensional changes of glulam was developed by reflecting the nonlinear behavior of shrinkage based on MC change. It was compared with the existing method provided by the American Wood Council (AWC). Moisture-related strains of glulam were significantly influenced by size and species. Coefficients of swelling or shrinkage of glulam were determined to indicate statistical significance. When MC was changed from saturated condition to EMC of 12%, differences in dimensional changes in the width direction between experimental test and prediction results using the AWC method ranged from 87.7% to 260.0%. However, differences in dimensional changes in the width direction between experimental test and prediction results using the newly developed method ranged from 1.8% to 15.9%. Strains in the width direction of glulam could be affected by adjacent laminas along the glue line and the new approach could account for the effects. However, the AWC method could not reflect the effects of adjacent laminas along the glue line. Therefore, better prediction accuracy was achieved by using the new approach.

Keywords: Glulam, coefficient, swelling, shrinkage, digital image correlation, moisture content.

INTRODUCTION

Glued–laminated timber (glulam) is a structurally engineered wood product made by a number of laminas glued together lengthwise (Yang et al 2009; Cheng and Hu 2011). A 1% change in MC of wood has a 10 times greater effect on the dimensional change than a 1°C change in temperature (Gereke et al 2009). Dimensional changes should be considered for structural design of wooden building (AWC 2015a). The lamina in glulam is a solid wood. Dimensional changes of glulam are also critically influenced by MC changes.

Dimensional changes of wood by MC can occur under FSP until wood reaches the EMC (Choong and Achmadi 2007). Several studies (Stohr 1988; Peng et al. 2012; Lee and Jeong 2018) have revealed that the shrinkage rate of wood is decreased when the specimen size is increased. Silva et al (2014) have studied hygroscopic behaviors of three softwood species by changing the

* Corresponding author
† SWST member

Wood and Fiber Science, 51(2), 2019, pp. 101-118
https://doi.org/10.22382/wfs-2019-013

MC. Linear shrinkage and expansion of maritime pine (*Pinus pinaster*), spruce (*Picea abies*), and scots pine (*Pinus sylvestris*) were determined. Shrinkage was observed to be higher than swelling. Changed size of wood at different EMC can be calculated using coefficients for moisture expansion and shrinkage. Shrinkage coefficients of wood are based on oriented small wood specimens (ISO/TC 1982a, 1982b; ASTM 2014).

Dimensional changes of glulam can also be calculated using coefficients for wood (APA 1998; AWC 2015b). However, the cross section of glulam is composed of laminas with random growth ring patterns. Such random growth ring patterns indicate that shrinkage and swelling of glulam would be different from those of the solid wood. Therefore, shrinkage and swelling behaviors of glulam would be different from those of a small clear sample.

Moisture-related strain of glulam has been investigated by cutting an inner slice from the actual glulam (Jonsson and Svensson 2004; Anges and Malo 2012) or simulated by numerical approaches (Zhou et al 2010; Fragiacomo et al 2011). Jonsson and Svensson (2004) have cut a Norway spruce glulam (cross section: 90 $\times$ 270 mm^2) into 11 slices to evaluate the internal stress in glulam depending on MC changes. Anges and Malo (2012) have also used 90-mm thickness specimens cut from a specific EMC glulam to investigate moisture-induced stresses of glulam. Zhou et al (2010) have developed a sequentially coupled three-dimensional (3D) finite element procedure to investigate hygrothermal stress in glulam beams. Fragiacomo et al (2011) have used a finite element model to simulate the MC and stress distribution on different sizes of timber exposed to climatic regions.

Recently, digital image correlation (DIC) has been applied to investigate the displacement of wood. DIC is a contactless deformation measuring method. It can track two-dimensional (2D) or 3D displacements of a specimen under different loading conditions (Jeong and Park 2016). The high accuracy and high repeatability of DIC method have been revealed by several researchers. Jeong et al (2009) have measured elastic properties and strength of loblolly pine using DIC. Jeong et al (2010) have investigated effects of different specimen thicknesses and loading rates on measurement of Young's modulus and Poisson's ratio by DIC. Hansmann et al (2011) have performed digital image analyses to determine dimensional changes of Norway spruce along the whole moisture range. Keunecke et al (2012) have tried to evaluate 2D data generated with X-ray and DIC to analyze moisture-induced strain in wood. They revealed that several issues (species, shear deformation, local properties, etc.) should be solved to enhance its effectiveness and user-friendliness. Xavier et al (2012) have measured the strain of maritime pine (*Pinus pinaster* Ait.) in compression tests using DIC and glued strain gauges. They revealed that DIC method provided similar results compared with strain gauge measurements.

The aim of this study was to investigate moisture-related strains of different sized glulam made from larch (*Larix kaempferi*) and pine (*Pinus koraiensis*) using DIC. Effects of size and species on swelling and shrinkage of glulam were statistically analyzed. Coefficients of swelling and shrinkages of different sized glulams made from two species were determined. A new method was suggested to predict dimensional changes of glulam according to the MC.

MATERIALS AND METHODS

Materials

Different sized (120 $\times$ 120 $\times$ 120, 180 $\times$ 180 $\times$ 180, and 180 $\times$ 240 $\times$ 180 mm^3) glulam made from larch (density for larch glulam: 500 kg/m^3) and pine (density for pine glulam: 420 kg/m^3) were prepared to measure swelling and shrinkage. The density vlaues were obtained when the volume of glulam at 12% MC was divided by oven-dry weight. To measure swelling and shrinkage values in width, depth, and length of different sized glulam, 15 specimens were prepared for each condition. Width and depth

directions were defined in perpendicular to the length. Width direction in cross section of glulam was parallel to the glue line, whereas the depth direction in cross section of glulam was perpendicular to the glue line.

Conditioning of Different Sized Glulam

To simulate swelling and shrinkage of different sized glulam, an environmental chamber (VS-9111H-350; Vison Science Co. Bucheon, South Korea) was used to condition the temperature and RH. Figure 1 shows the process of conditioning steps used in swelling and shrinkage measurement. The swelling of different sized glulam was determined from an EMC of 6% to saturated MC. All specimens were immersed in water for 12 wk to reach saturation.

Shrinkage of different sized glulam was determined from saturated condition to oven-dried condition. All specimens were conditioned in an environmental chamber with different RHs at 30°C to reach an EMC of 19%, 12%, and 8%. For specimens to reach an EMC of 19%, 12%, and 8%, 7 wk, 4 wk, and 2 wk were needed, respectively. After reaching an EMC of 8%, all specimens were put in an oven for 4 wk. Each different conditioning period was determined by comparing changes in weight and dimension of specimen every 3 d. If weight and dimension of specimens were changed by less than 0.5%, measurement of dimension for each condition was taken before proceeding to the next condition.

The actual MC of specimen was calculated using specimen weight at target condition and specimen weight after oven-dried condition according to ASTM D 4442 (ASTM 2007). A digital balance (HS 2100F; Hangung Co., Seoul, South Korea) of sensitivity of 0.01 g was used to measure the specimen weight.

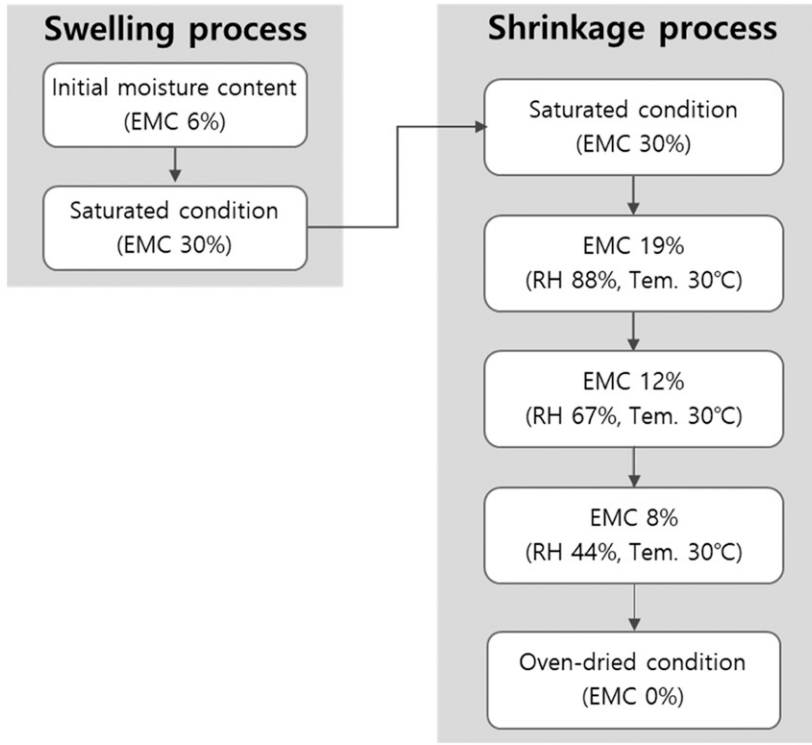

Figure 1. Process of conditioning glulam to measure coefficients of moisture expansion and shrinkage. Tem., temperature.

Measurement of Dimensional Changes

Dimensional changes from an EMC of 6% to saturated condition were measured using a digital caliper. The sensitivity of the digital caliper was 10 μm. Dimensions of the width, depth, and length were measured along the measurement line between two conditions. Dimensional changes from saturated condition to oven-dried condition were also measured using a digital caliper with DIC technique.

Figure 2 shows the test setup to capture images of different sized glulam for DIC. A metal fixture was designed to fix a camera and distance between different sizes of three objects and lenses to ensure the field of view. To capture the surface image of glulam with different EMC conditions, a digital camera (Nikon D810; Nikon Co., Japan) with 60-mm micro lenses (Nikon AF-S Micro NIKKOR 60 mm f.2.8G ED) was used. Image resolution of the camera was 7360 × 4912 pixel. For 120 × 120, 180 × 180, and 180 × 240-mm glulam, pixel dimensions were 17.66 μm/pixel × 26.47 μm/pixel, 24.45 μm/pixel × 36.64 μm/pixel, and 32.60 μm/pixel × 36.64 μm/pixel, respectively.

To reduce vibration and maintain the same image quality, the camera was connected to a notebook and controlled with Camera Control Pro2 2.19 software (Nikon Co., Japan). Surface images of different sized glulam under different conditions were captured with the following setting: shutter speed of 1/5 s, F/5, and ISO of 100.

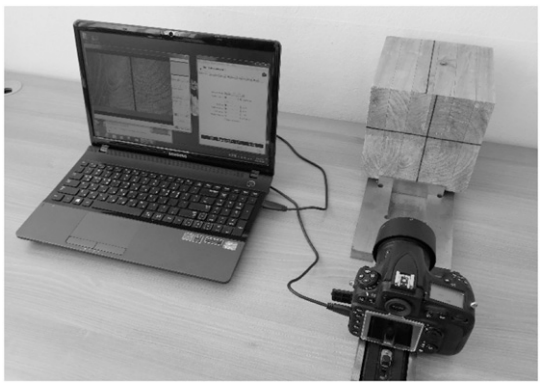

Figure 2. Setup for digital image correlation showing computer operating a camera to take picture of the surface of the sample mounted onto a metal fixture.

Shrinkage of Different Sized Glulam Using DIC

DIC was conducted using ARAMIS v6.3 (GOM mbH 2011; Braunschwig, Germany). Surface images of glulam from saturated MC to oven-dried condition were used (Fig 3). After calibrating different facet sizes (60, 80, 100, 120, 140, 160, 180, and 200) and facet steps (30, 40, 50, 60, 70, 80, 90, and 100), facet size of 200 and facet step of 50 were defined to measure shrinkage of glulam for all specimens under different MCs. Using DIC, shrinkage distribution of different size glulam was analyzed and shrinkage values along the path in width and depth direction were measured for all specimen. Because of the space, the strain distribution and strain values from different sizes of glulam from one specimen were shown in Figs 6-8, 10, and 11.

Effects of Species and Size on Swelling and Shrinkage of Glulam

Effects of species and size on swelling and shrinkage of glulam were analyzed using the two-way analysis of variance. For the analysis, statistic program (SAS 9.4; SAS Institute Inc., NC) was used. Significant difference was set at $\alpha = 0.05$. If p-value was under 0.05, the difference between groups was considered statistically significant. Swelling values of the same sized glulam made from larch and pine were compared. Shrinkage values of the same sized glulam made from larch and pine were also compared. To determine the effect of size on swelling and shrinkage, swellings or shrinkages of different sized (120 × 120 × 120, 180 × 180 × 180, and 180 × 240 × 180 mm^3) glulam in the same direction made of the same species were compared.

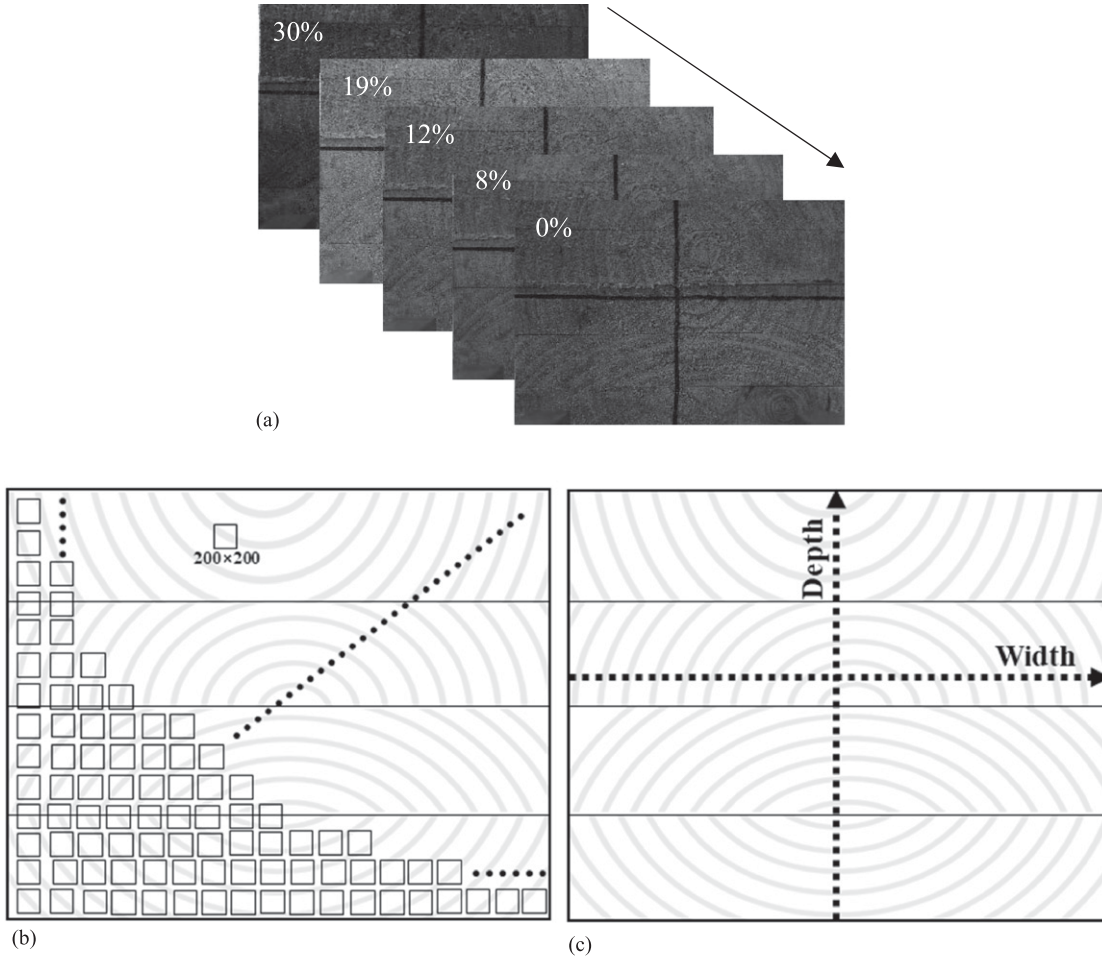

Figure 3. Process of digital image correlation to analyze strain distribution and strain values along a path. (a) Surface images at different MC, (b) virtual grids, (c) paths in width and depth.

RESULTS AND DISCUSSION

Swelling Coefficients of Glulam Depending on Species, Sizes, and Directions

Effects of size and species on moisture-related strain were determined by comparing swelling and shrinkage coefficients depending on material directions of glulam. Swelling coefficients depending on material directions were derived from the relationship between averages of strain distributions obtained from DIC as MC changed from EMC of 6% to saturated MC (Fig 4). In the swelling process, glulam specimens were immersed in water to make them saturated. There was no intermediate point. Thus, swelling coefficients were assumed to be linear. Swelling coefficients in width and depth directions of larch glulam were about 0.0010 and ranged from 0.0008 to 0.0013, respectively. Swelling coefficients in width and depth directions for pine glulam ranged from 0.0004 to 0.0007 and from 0.0004 to 0.0007, respectively. In the length direction, the swelling coefficients for larch glulam at a size of 120 × 120, 180 × 180, and 180 × 240 mm^2 were 0.00005, 0.00004, and 0.00004, respectively. Swelling coefficients for pine glulam at a size of 120 × 120, 180 × 180, and 180 × 240 mm^2 were 0.00004, 0.00005, and

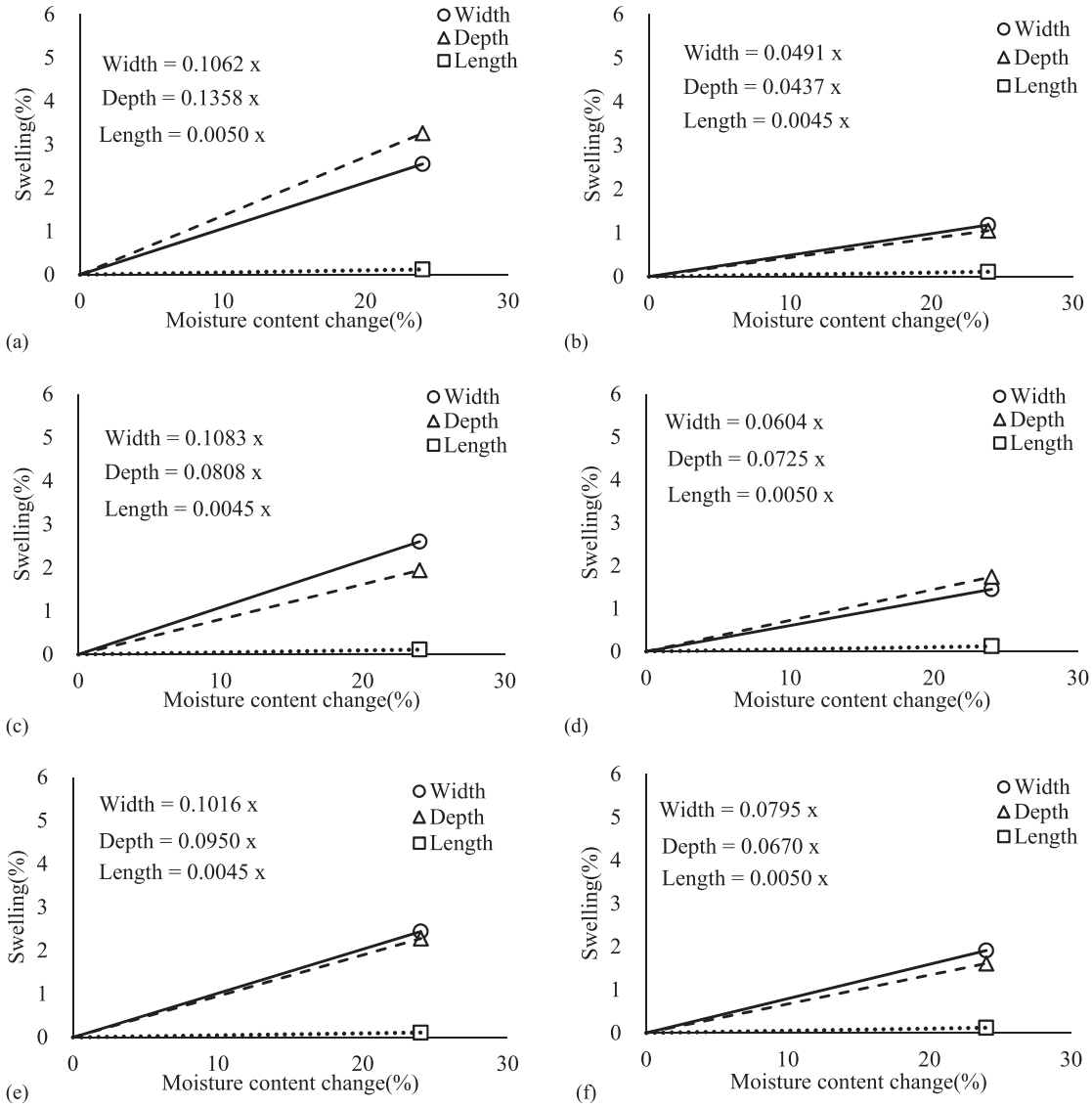

Figure 4. Swelling of specimens when the MC was changed from 6% to saturated condition. (a) Larch glulam at size of 120 × 120 mm^2, (b) pine glulam at size of 120 × 120 mm^2, (c) larch glulam at size of 180 × 180 mm^2, (d) pine glulam at size of 180 × 180 mm^2, (e) larch glulam at size of 180 × 240 mm^2, (f) pine glulam at size of 180 × 240 mm^2. (Note: the point indicates the average value.)

0.00005, respectively. The swelling in the length direction was 10 times lower than that in width and depth directions regardless of size or species.

Statistical analysis (Table 1) showed that the species significantly influenced the swelling of glulam in width and depth directions. Based on statistical analysis results, swelling coefficients of glulam were determined (Table 2). Dimensional changes (D_{swelling}) by MC change (ΔM) can be calculated using the derived swelling coefficients (β_{swelling}) and Eq 1 (AWC 2015b).

$$D_{\text{swelling}} = D_{\text{i}} \cdot \beta_{\text{swelling}} \cdot \Delta M, \qquad (1)$$

Table 1. Statistical analysis for effects of species and size on swelling and shrinkage of specimens ($\alpha = 0.05$).

	Swelling		Shrinkage	
	Source	*p*-value	Source	*p*-value
Width	Species	*<0.0001*	Species	0.6588
	Size	0.5043	Size	0.0741
Depth	Species	*<0.0001*	Species	*0.0013*
	Size	0.3755	Size	*0.0363*
Length	Species	0.5309	Species	*<0.0001*
	Size	0.9725	Size	*0.0015*

Note: The significance value shown in italized.

where $D_{swelling}$ is the dimensional changes by swelling, D_i is the dimension at the initial condition, $\beta_{swelling}$ is the swelling coefficient, and ΔM is the MC change.

Slope of Shrinkage for Glulam Depending on Species, Size, and Direction

In the shrinking process, the shrinkage of glulam showed nonlinear behavior as the MC changed from saturated condition (30%) to oven-dried condition (0%) (Fig 5). This phenomenon was similar to previouly reported results of different wood species by USDA (2010). The shrinkage–MC change curve needs to be a quadratic function to reflect experimental results. To fit the curve to a quadratic function, the slope of shrinkage was derived as a function of MC change (Eq 2). The saturated condition of specimens was assumed to 30% MC. MC changes should be calculated from 30% to MC at specific moisture condition (M_s) (Eq 2).

$$\beta_{shrinkage} = a(30 - M_s) + b, \quad (2)$$

where $\beta_{shrinkage}$ is the coefficient of shrinkage, M_s is the specific MC, and a and b are the constants derived by experimental test.

To calculate dimensional change ($D_{shrinkage}$) in shrinkage, the shrinkage calculated from the saturated condition to the initial condition should be excluded from the shrinkage calculated from the saturated condition to the final condition (Eq 3).

$$D_{shrinkage} = D_i[\beta_e(30 - M_e) - \beta_i(30 - M_i)], \quad (3)$$

where $D_{shrinkage}$ is the dimensional change by shrinkage, D_i is the dimension at the initial condition, β_e is the shrinkage coefficient at the final condition, M_e is the MC at the final condition, β_i is the shrinkage coefficient at the initial condition, and M_i is the MC at the initial condition.

Results of statistical analysis (Table 1) for shrinkage showed that both species and size significantly influenced depth and length directions of glulam. Based on these results, shrinkage coefficients of glulam were determined (Table 2). A negative shrinkage (ie swelling) in the length direction was observed (Fig 6). In the case of solid wood, longitudinal swelling behavior has been observed even when wood is dried (Welch 1932; Cockrell 1943; Hann 1969). From a mechanical point of view, when uniaxial stress happens, a negative strain should be happened in the transverse direction because of Poisson's ratio (Chen and He 2017). The swelling in the length direction

Table 2. Coefficients of moisture expansion and slope of moisture shrinkage of specimens.

		Coefficient of moisture expansion		The slope of moisture shrinkage	
Direction	Size (mm^2)	Larch	Pine	Larch	Pine
Width	120 × 120	0.0010	0.0006	$0.0045\Delta M - 0.0086$	
	180 × 180				
	180 × 240				
Depth	120 × 120	0.0013	0.0004	$0.0046\Delta M - 0.0218$	$0.0043\Delta M - 0.0333$
	180 × 180	0.0008	0.0006	$0.0029\Delta M + 0.0448$	$0.0037\Delta M - 0.0077$
	180 × 240				
Length	120 × 120	0.00004		$0.0004\Delta M - 0.0278$	$0.0006\Delta M - 0.0115$
	180 × 180				
	180 × 240			$-0.0006\Delta M + 0.0152$	

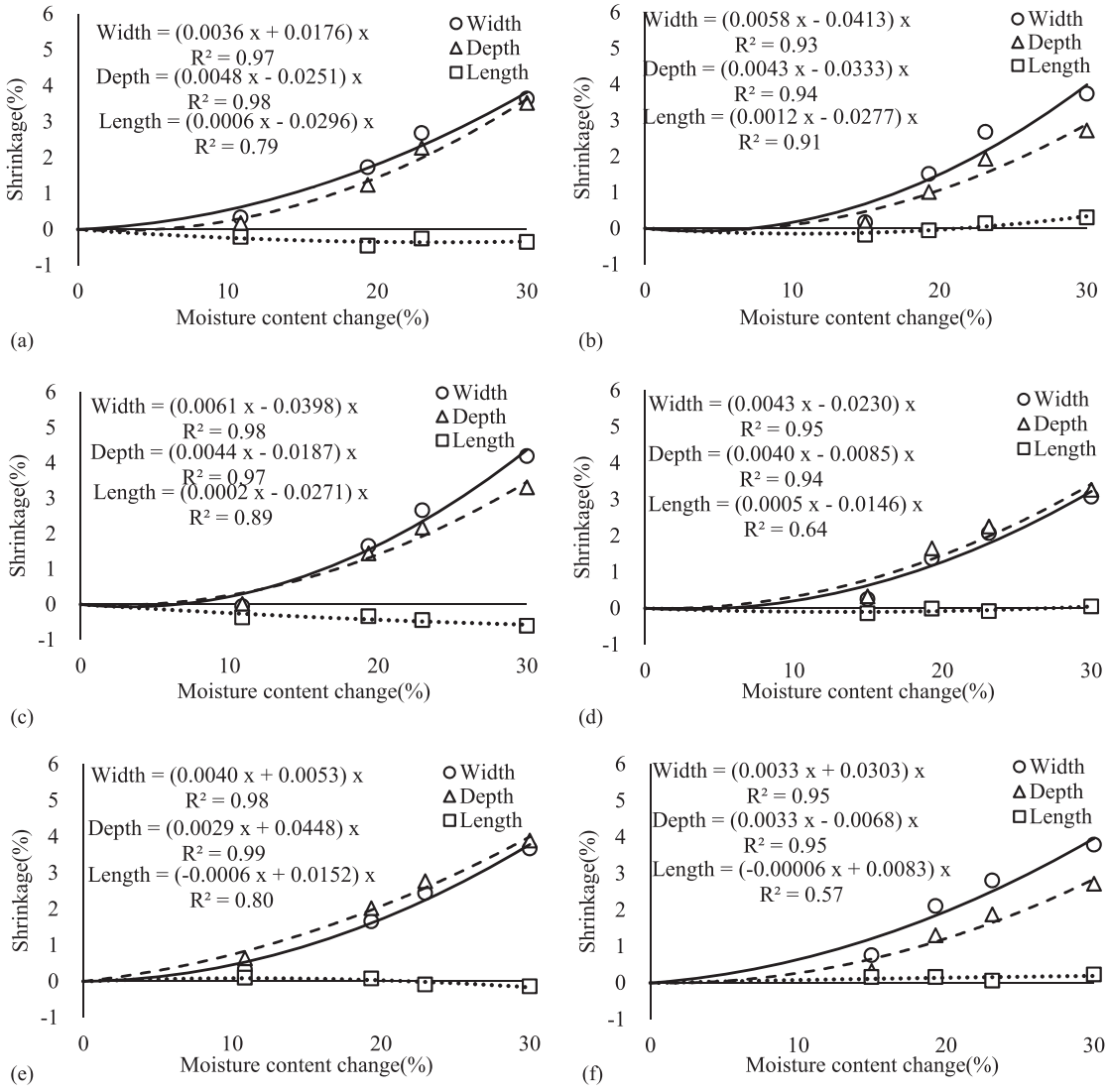

Figure 5. Shrinkage of different sized specimens when the MC was changed from saturated to oven-dried condition. (a) Larch glulam at size of 120 × 120 mm^2, (b) pine glulam at size of 120 × 120 mm^2, (c) larch glulam at size of 180 × 180 mm^2, (d) pine glulam at size of 180 × 180 mm^2, (e) larch glulam at size of 180 × 240 mm^2, (f) pine glulam at size of 180 × 240 mm^2. (Note: The point indicates the average value.)

could be caused by high shrinkage in width and depth directions.

Moisture-Related Strain Distribution

The slope of shrinkage shown in Table 2 was derived from the average of strain distributions obtained from DIC. Figure 7 shows shrinkage strain distribution in the width direction due to shrinkage from the saturated condition to the oven-dried condition. For larch glulam at a size of 120 × 120, 180 × 180, and 180 × 240 mm^2, maximum strain values were −9.824%, −9.926%, and −9.255%, respectively. For pine glulam at a size of 120 × 120, 180 × 180, and 180 × 240 mm^2, maximum strain values were −10.220%, −8.075%, and −10.870%, respectively.

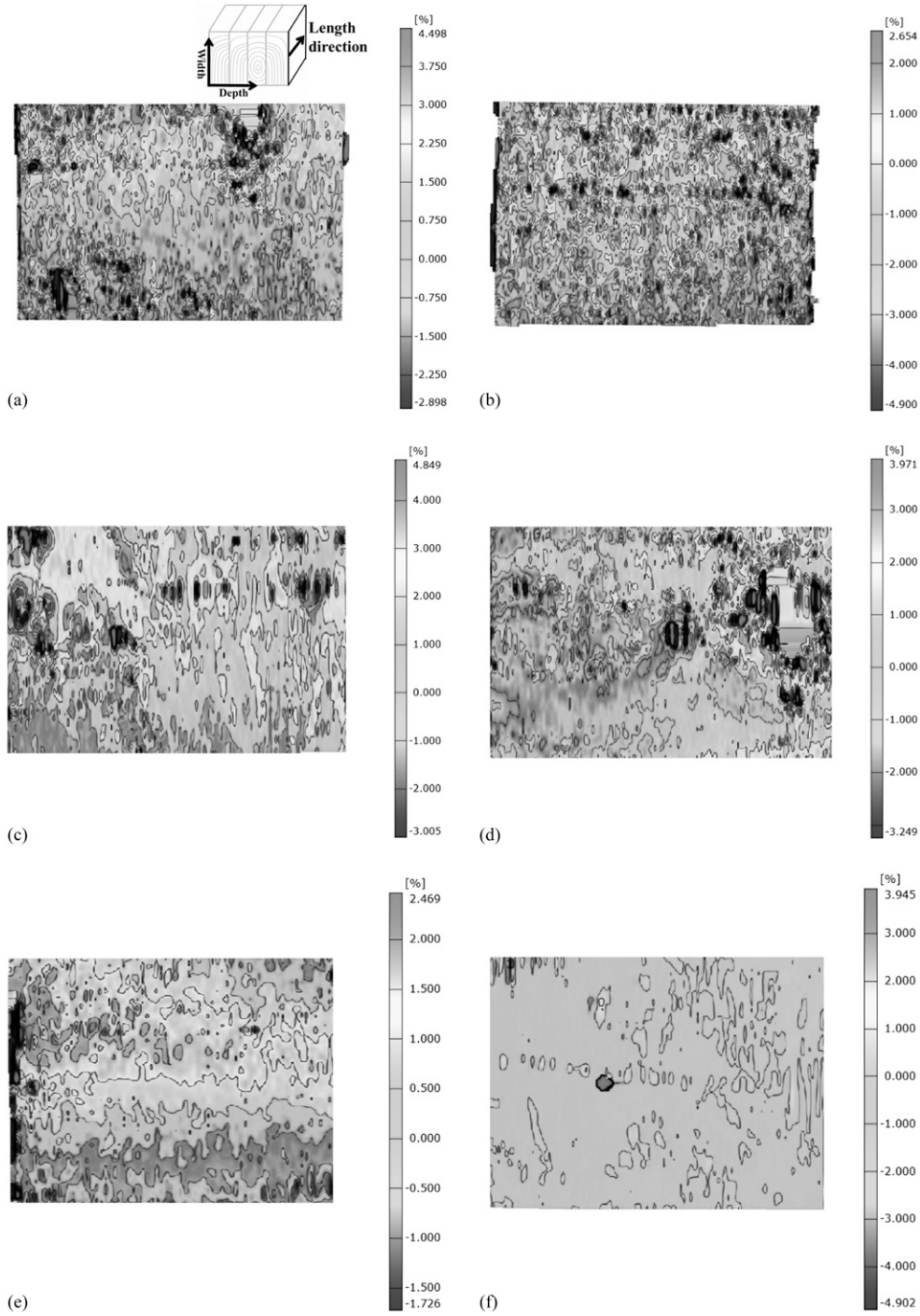

Figure 6. Strain distribution of specimens in the length direction by shrinkage from saturated to oven-dried condition. (a) Larch glulam at size of 120 × 120 mm^2, (b) pine glulam at size of 120 × 120 mm^2, (c) larch glulam at size of 180 × 180 mm^2, (d) glulam at size of 180 × 180 mm^2, (e) larch glulam at size of 180 × 240 mm^2, (f) pine glulam at size of 180 × 240 mm^2. (Note: Each graph is for one specimen that show the strain distribution in each condition.)

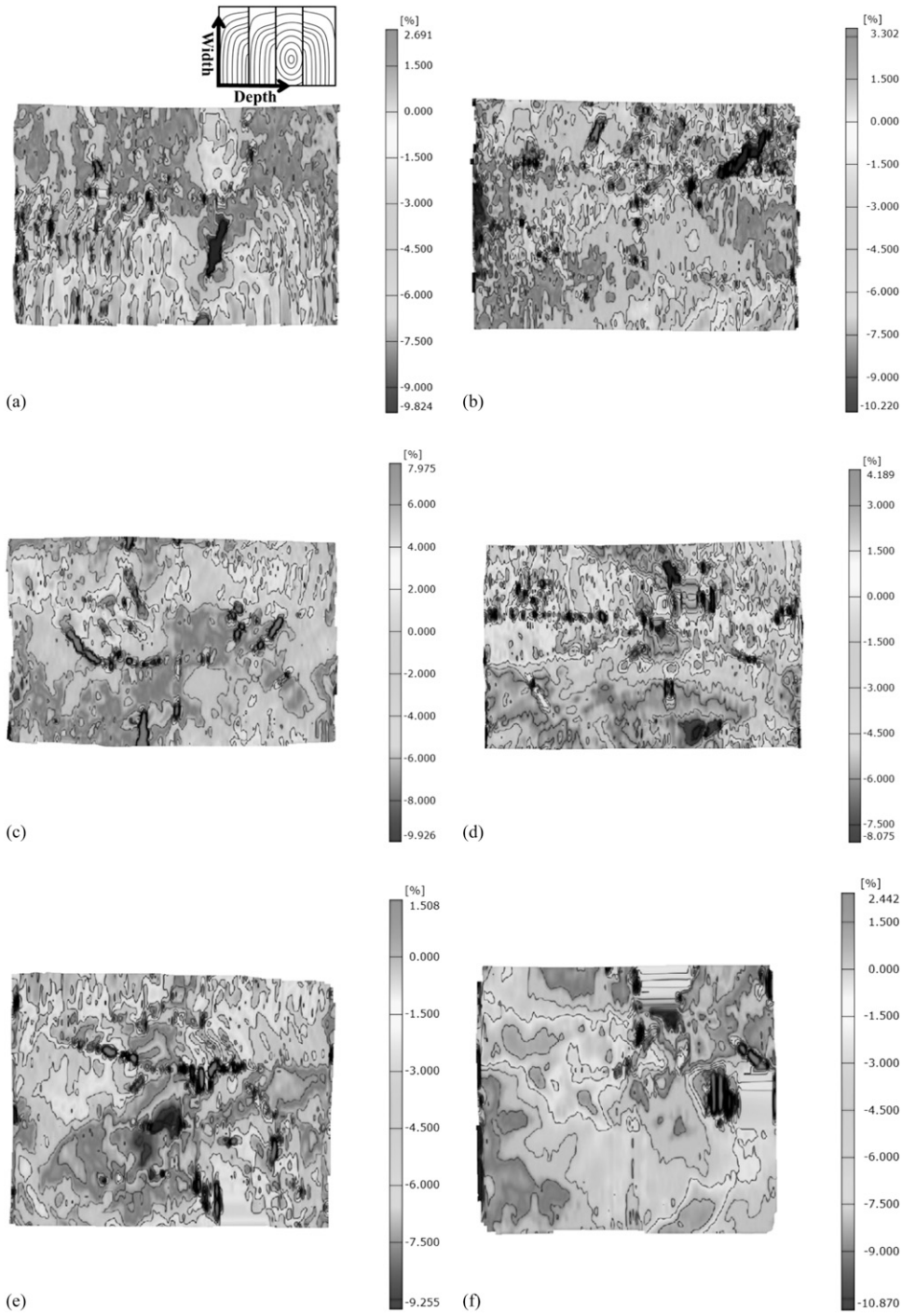

Figure 7. Strain distribution of specimens in the width direction by shrinkage from saturated to oven-dried condition. (a) 120 × 120 mm^2 for larch glulam, (b) 120 × 120 mm^2 for pine glulam, (c) 180 × 180 mm^2 for larch glulam, (d) 180 × 180 mm^2 for pine glulam, (e) 180 × 240 mm^2 for larch glulam, (f) 180 × 240 mm^2 for pine glulam. (Note: Each graph is for one specimen that show the strain distribution in each condition.)

Wood is an inhomogeneous material. Therefore, strain distribution in glulam was different, depending on localized properties. To determine characteristics of localized strains in the width direction, strain distributions along a path were derived. Figure 8 shows localized strain distribution when specimens reached several EMC conditions from the saturated condition. The

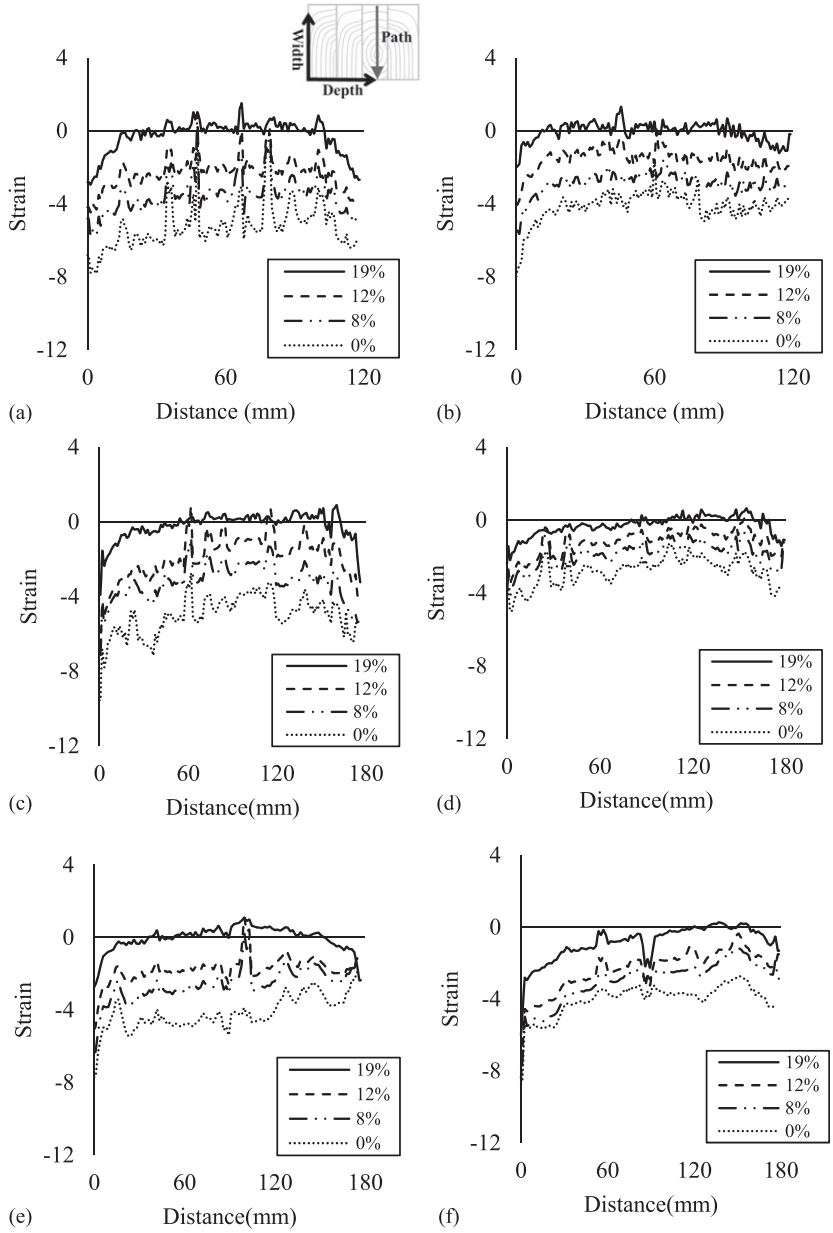

Figure 8. Strain values of specimens in the width direction along the path when MC was changed from saturated to oven-dried condition. (a) Larch glulam at size of 120 × 120 mm^2, (b) pine glulam at size of 120 × 120 mm^2, (c) larch glulam at size of 180 × 180 mm^2, (d) pine glulam at size of 180 × 180 mm^2, (e) larch glulam at size of 180 × 240 mm^2, (f) pine glulam at size of 180 × 240 mm^2. (Note: Each graph is for one specimen that show the strain distribution in each condition.)

pattern of the localized strain distribution showed that each localized strain varied depending on localized properties. Difference between earlywood and latewood in a growth ring clearly appeared in the localized strain distribution. When specimens were dried to lower EMC conditions, localized strains became higher. However, the strain distribution pattern was not significantly changed. In other words, when the EMC of specimen became lower, the localized strain values were generally increased while maintaining the relative strain difference.

When a wood is dried, negative strain (ie swelling) in cross section has been reported by Clair et al (2003) and Silva et al (2014). In this study, small negative strains also occurred in some specimens when the MC of specimens was changed from 30% to 19%. The cross section of glulam is composed of various laminas with different growth ring patterns. A flat distortion of lamina occurred by shrinkage due to direction of growth rings (Fig 9). Shrinkage in the tangential direction is known to be twice as great as the shrinkage in the radial direction (Hernandez and Pontin 2006; Hernandez 2007; USDA 2010). Because of distortion of a lamina, the compression force or tension force will lead to laminas glued on the side. An expansion can occur on the tension side of a flat distortion lamina, although the glulam is shrinking. On the contrary, a lamina on the compression side of the flat distortion lamina will shrink further. This phenomenon occurs along the glue line because laminas are glued to each other. If the glue line could not transmit the tensile or compressive force, this phenomenon would not have occurred. This phenomenon can be called a glue line effect.

Although this phenomenon can be caused by adjacent laminas, distortion of one lamina is restricted by other laminas in the glulam. Several laminas are in glulam and each lamina is glued on the wide face. Small negative strains appeared locally when glulam was dried from saturated condition to 19%. The overall dimensional change was small compared with other stages of shrinkage. However, when the EMC of specimens reached 12% or lower, expansion strains became shrinkage strains, whereas overall dimensions were reduced.

Compared with strain distribution in the width direction, difference in strain distribution between laminas appeared in the depth direction (Fig 10). Again, the glue line between laminas appeared clearly in the strain distribution of the depth direction. Figure 10 shows strain distributions in the depth direction when the MC was changed from 30% to 0%. For larch glulam at a size of 120 × 120, 180 × 180, and 180 × 240 mm^2, the maximum strains were −9.716%, −10.102%, and −11.313%, respectively. For pine glulam at a size of 120 × 120, 180 × 180, and 180 × 240 mm^2, maximum strain values were −7.046%, −9.543%, and −8.761%, respectively.

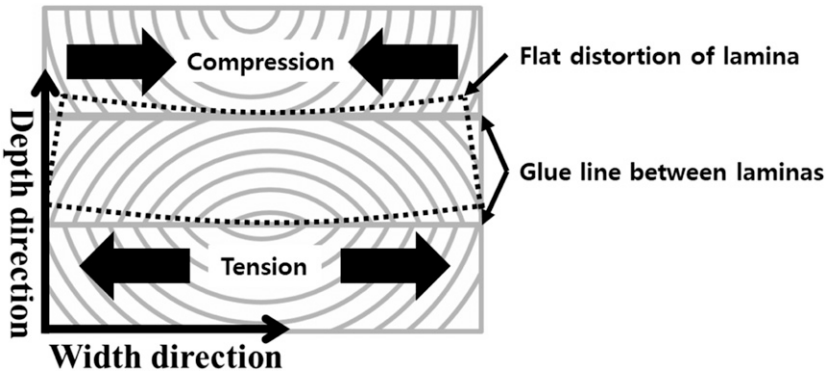

Figure 9. Compression and tension due to distortion of a lamina in glulam.

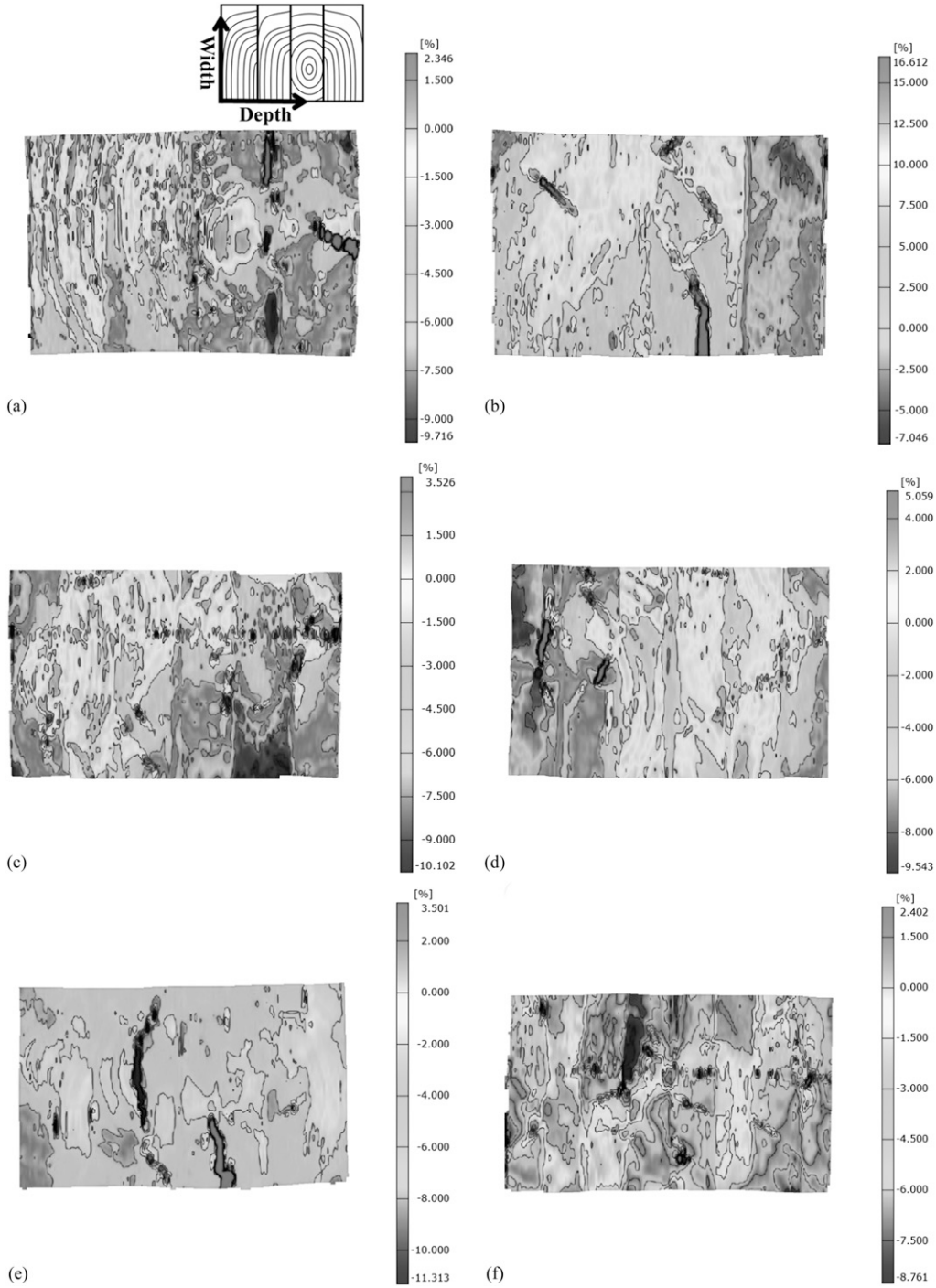

Figure 10. Strain distribution of specimens in the depth direction by shrinkage from saturated to oven-dried condition. (a) Larch glulam at size of 120 × 120 mm^2, (b) pine glulam at size of 120 × 120 mm^2, (c) larch glulam at size of 180 × 180 mm^2, (d) pine glulam at size of 180 × 180 mm^2, (e) larch glulam at size of 180 × 240 mm^2, (f) pine glulam at size of 180 × 240 mm^2. (Note: Each graph is for one specimen that show the strain distribution in each condition.)

Figure 11 shows localized strain distributions along a path in the depth direction according to MC changes. Variations within lamina and among laminas appeared in localized strain distributions. The variation among laminas was greater than that within a lamina. In the width direction, negative strains also occurred when the EMC of specimens reached 19%. Negative strains became shrinkage strains when the EMC of specimens reached 12% or lower. These

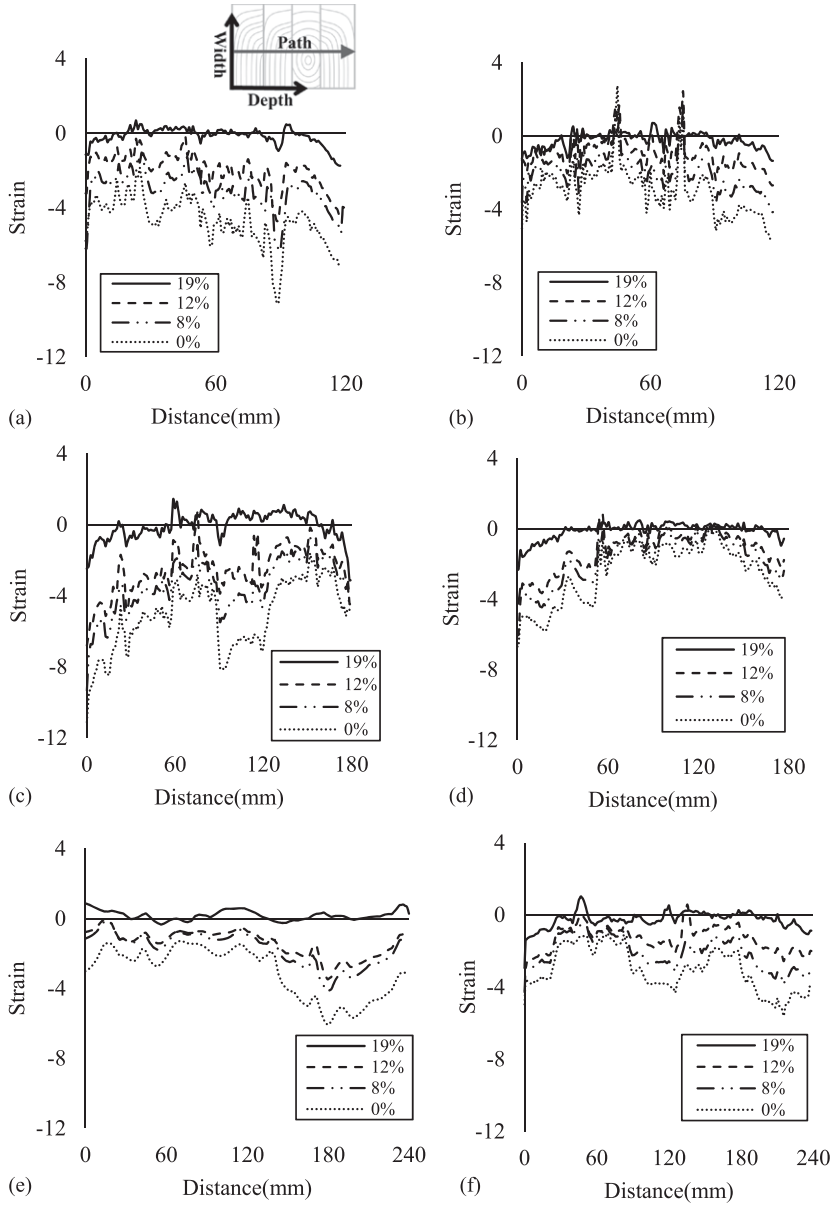

Figure 11. Strain values of specimens in the depth direction along the path when the MC was changed from saturated to oven-dried condition. (a) Larch glulam at size of 120 × 120 mm^2, (b) pine glulam at size of 120 × 120 mm^2, (c) larch glulam at size of 180 × 180 mm^2, (d) pine glulam at size of 180 × 180 mm^2, (e) larch glulam at size of 180 × 240 mm^2, (f) pine glulam at size of 180 × 240 mm^2. (Note: Each graph is for one specimen that show the strain distribution in each condition.)

localized strain patterns generally maintained as the EMC of specimens became lower. This indicates that the moisture in specimens is equally reduced at all localized areas.

Differences between Predicted Strains and Measured Strains

Predicted dimensional changes and the slope of shrinkage were compared with measured values and other predicted values by the existing method in AWC (2015b). The equation in AWC (2015b) is the same as Eq 1. Tangential and radial coefficients were used to predict dimensional changes of glulam (APA 1998). Coefficients of tangential and radial directions were selected considering species and density of tested specimens. Coefficients for Douglas fir-larch (density: 500 kg/m^3) were applied for larch glulam (0.0033 for width direction and 0.0018 for depth direction). Coefficients for redwood (density: 440 kg/m^3) were applied for pine glulam (0.0022 for width direction and 0.0012 for depth direction). Dimensional changes in the length direction could not be derived because of no coefficient in the length direction in AWC (2015b).

Table 3 shows the differences between predicted dimensional changes and measured values. When the MC was changed from the saturated condition to 12% EMC, differences between predicted values by the new approach and measured values were 1.8-15.9% in the width direction and 2.5-18.2% in the depth direction. Differences between predicted values by the AWC method and measured values were 87.7-260.0% in the width direction and 30.9-161.3% in the depth direction. When the MC was changed from the saturated condition to 8% EMC, differences between predicted values by the new approach and measured values were 4.8-26.5% in the width direction and 6.9-16.7% in the depth direction. Differences between predicted values by the AWC method and measured values were 72.2-197.5% in the width direction and 17.3-82.5% in the depth direction. These results showed that predicted values by the new approach agreed with measured values better than predicted values by the existing method in AWC. The more accurate prediction with the new approach might be due to the following. First, nonlinear shrinkage behavior was reflected as a slope of shrinkage by the new approach when the MC was decreased. Second, random growth ring patterns were reflected in the new approach because the slope of shrinkage was derived from the actual size of glulam. However, it is difficult to reflect the random orientation of growth ring in glulam with the existing AWC method.

In the width direction of glulam, the shrinkage of a lamina was restricted by adjacent laminas because laminas were glued to each other. This phenomenon did not occur if the adhesive layer between laminas could not support the shear force generated by different shrinkages between laminas. The AWC method cannot reflect this phenomenon because this method predicts dimensional change of glulam by shrinkage coefficients of individual laminas. Dimensional changes predicted by the AWC method were quite different from measured values in the width direction. The AWC method showed better prediction accuracy in the depth direction than that in the width direction. In the depth direction of glulam, the shrinkage of each lamina was not affected by the shrinkage of other laminas because there was no glue line. Therefore, dimensional changes in the depth direction of glulam were similar to those in the radial direction for individual lamina. However, dimensional changes in the width direction of glulam were not similar to those in the tangential direction of individual lamina because of the glue line effect.

CONCLUSIONS

In this study, effects of size and species on moisture-related strains of glulam were analyzed and a new approach was suggested to predict dimensional changes of glulam according to the MC. Statistical analysis results showed that moisture-related strains of glulam were significantly influenced by size and species. Swelling and shrinkage in width and depth directions were significantly influenced by species. Shrinkage in the depth direction was significantly influenced

Table 3. Differences in dimensional changes predicted by the new approach and the AWC method.

Species	Dimension (mm)			Reached EMC from saturated condition (%)	Measured dimensional change (mm)			Predicted dimensional change (mm)				
								New approach[a]			AWC[b]	
	Width	Depth	Length		Width	Depth	Length	Width (dif.)[c]	Depth	Length	Width[d]	Depth[e]
Larch	120	120	120	12	2.08	1.49	−0.55	1.94 (6.4%)	1.60 (7.3%)	−0.46 (17.4%)	7.13 (243.4%)	3.89 (161.3%)
				8	3.22	2.72	−0.31	2.77 (13.8%)	2.27 (16.7%)	−0.50 (61.5%)	8.71 (170.9%)	4.75 (74.4%)
	180	180	180	12	2.97	2.59	−0.61	2.92 (1.8%)	2.39 (7.6%)	−0.68 (11.8%)	10.69 (260.0%)	5.83 (125.0%)
				8	4.79	3.91	−0.81	4.16 (13.2%)	3.40 (12.9%)	−0.76 (6.7%)	13.07 (172.9%)	7.13 (82.5%)
	180	240	180	12	2.99	4.85	0.14	2.92 (2.4%)	4.73 (2.5%)	0.07 (50.0%)	10.69 (257.8%)	7.78 (60.4%)
				8	4.39	6.65	−0.16	4.16 (5.3%)	6.19 (6.9%)	−0.02 (88.9%)	13.07 (197.5%)	9.50 (43.0%)
Pine	120	120	120	12	1.81	1.21	−0.07	1.52 (15.9%)	1.42 (16.8%)	−0.08 (16.7%)	4.75 (162.3%)	2.59 (113.9%)
				8	3.22	2.32	0.17	2.36 (26.5%)	2.03 (12.4%)	0.00 (100.0%)	5.81 (80.6%)	3.17 (36.8%)
	180	180	180	12	2.47	2.97	−0.02	2.29 (7.3%)	2.43 (18.2%)	−0.13 (600.0%)	7.13 (189.1%)	3.89 (30.9%)
				8	3.73	4.05	−0.14	3.55 (4.8%)	3.58 (11.6%)	0.00 (100.0%)	8.71 (133.8%)	4.75 (17.3%)
	180	240	180	12	3.80	3.14	0.29	3.33 (12.3%)	2.71 (13.7%)	0.25 (12.5%)	7.13 (87.7%)	5.18 (64.9%)
				8	5.06	4.51	0.11	4.52 (10.7%)	3.96 (12.2%)	0.29 (166.7%)	8.71 (72.2%)	6.34 (40.4%)

[a] Calculated from Eq 2 and the slope of shrinkage in Table 2.
[b] Calculated from Eq 1 and shrinkage coefficients in AWC (2015b).
[c] Difference between predicted and measured shrinkages $= \left|\frac{\text{Predicted value} - \text{Measured value}}{\text{Measured value}}\right| \times 100$.
[d] 0.0033 (tangential coefficient of Douglas fir-larch) and 0.0022 (tangential coefficient of redwood) used for larch and pine, respectively.
[e] 0.0018 (radial coefficient of Douglas fir-larch) and 0.0012 (radial coefficient of redwood) used for larch and pine, respectively.
AWC, American Wood Council.

by size. Swellings of larch glulam in width and depth directions were higher than those of pine glulam. Compared with swelling values from the EMC of 6% to the saturated condition, shrinkage values from the saturated condition to the EMC of 6% were higher. Dimensional change in the length direction was affected by dimensional changes in width and depth directions. A negative dimensional change appeared in the length direction of specimens.

With the new approach, the nonlinear shrinkage behavior was reflected as a slope of shrinkage when the MC was decreased. Predicted values with the new approach based on the slope of shrinkage agreed with measured values better than predicted values with the existing AWC method. The AWC method uses tangential and radial coefficients of lamina to predict dimensional changes of glulam. Dimensional changes in the depth direction of glulam were similar to those in the radial direction of laminas. However, dimensional changes in the width direction of glulam were not similar to those in the tangential direction of laminas because of the effect of adjacent laminas along the glue line. Results from DIC showed that strain values in the width direction were dependent on characteristics of all layers because of the effect of adjacent laminas along the glue line. However, strain values in the depth direction were dependent on characteristics of a specific layer. Therefore, the AWC method can be used to predict dimensional change of glulam in the depth direction. In the width direction, better prediction accuracy can be achieved by using the new approach developed in this study.

ACKNOWLEDGMENT

This study was carried out with the support of Forest Science & Technology Projects (Project No. S121414L040110) provided by Korea Forest Service.

REFERENCES

Anges V, Malo KA (2012) The effect of climate variations on glulam–An experimental study. Eur J Wood Wood Prod 70:603-613.

APA (1998) Dimensional changes in structural glued laminated timber. EWS Y260. Engineered Wood Systems, Tacoma, WA.

ASTM (2007) Standard test methods for direct moisture content measurement of wood and wood-base materials. D 4442-07. American Society for Testing and Materials, West Conshohocken, PA.

ASTM (2014a) Standard test methods for small clear specimens of timber. D143-14. American Society for Testing and Materials, Philadelphia, PA.

ASTM (2014b) Standard test methods for density and specific gravity (relative density) of wood and wood-based materials. D 2395-14. West Conshohocken, PA.

AWC (2015a) National design specification (NDS) for wood construction 2015 edition. American Wood Council, Leesburg, VA.

AWC (2015b) Manual for engineered wood construction 2015 edition. American Wood Council, Leesburg, VA.

Chen G, He B (2017) Stress-strain constitutive relation of OSB under axial loading: An experimental investigation. BioResources 12(3):6142-6156.

Cheng F, Hu Y (2011) Nondestructive test and prediction of MOE of FRP reinforced fast-growing poplar glulam. Compos Sci Technol 71:1163-1170.

Choong ET, Achmadi SS (2007) Effect of extractives on moisture sorption and shrinkage in tropical woods. Wood Fiber Sci 23(2):185-196.

Clair B, Jaouen G, Beauchêne J, Fournier M (2003) Mapping radial, tangential and longitudinal shrinkages and relation to tension wood in discs of the tropical tree *Symphonia globulifera*. Holzforschung 57(6):665-671.

Cockrell RA (1943) Some observations on density and shrinkage of ponderosa pine wood. Am Soc Mech Eng Trans 65:729-739.

Fragiacomo M, Fortino S, Tononi D, Usardi I, Toratti T (2011) Moisture-induced stresses perpendicular to grain in cross-sections of timber members exposed to different climates. Eng Struct 33(11):3071-3078.

Gereke T, Schnider T, Hurst A, Niemz P (2009) Identification of moisture-induced stresses in cross-laminated wood panels from beech wood (*Fagus sylvatica* L.). Wood Sci Technol 43:301-315.

GOM mbH (2011) Aramis v6.3 and higher user manual-software. GOM mbH, Braunschwig, Germany.

Hann RA (1969) Longitudinal shrinkage in seven species of wood. Res. Note FPL-0203. U.S. Department of Agriculture, Forest Service, Forest Products Laboratory, Madison, WI.

Hansmann C, Konnerth J, Rosner S (2011) Digital image analysis of radial shrinkage of fresh spruce (*Picea abies* L.) wood. Wood Mater Sci Eng 6:2-6.

Hernandez RE (2007) Swelling properties of hardwoods as affected by their extraneous substances, wood density, and interlocked grain. Wood Fiber Sci 39(1):146-158.

Hernandez RE, Pontin M (2006) Shrinkage of three tropical hardwoods below and above the fiber saturation point. Wood Fiber Sci 38(3):474-483.

ISO/TC (1982a) Wood—Determination of volumetric shrinkage. 4858. International Organization for Standardization, Geneva, Switzerland.

ISO/TC (1982b) Wood—Determination of volumetric swelling. 4860. International Organization for Standardization, Geneva, Switzerland.

Jeong GY, Park MJ (2016) Evaluate orthotropic properties of wood using digital image correlation. Constr Build Mater 113:864-869.

Jeong GY, Zink-Sharp A, Hindman DP (2009) Tensile properties of earlywood and latewood from loblolly pine (*Pinus taeda*) using digital image correlation. Wood Fiber Sci 41:51-63.

Jeong GY, Zink-Sharp A, Hindman DP (2010) Applying digital image correlation to wood strands: Influence of loading rate and specimen thickness. Holzforschung 64: 729-734.

Jonsson J, Svensson S (2004) A contact free measurement method to determine internal stress states in glulam. Holzforschung 58:148-153.

Keunecke D, Novosseletz K, Lanvermann C, Mannes D, Niemz P (2012) Combination of X-ray and digital image correlation for the analysis of moisture-induced strain in wood: Opportunities and challenges. Eur J Wood Wood Prod 70(4):407-413.

Lee SS, Jeong GY (2018) Effects of sample size on swelling and shrinkage of *Larix kaempferi* and *Crytomeria japonica* as determined by digital caliper, image analysis, and digital image correlation (DIC). Holzforschung 72:477-488.

Peng M, Ho YC, Wang WC, Chui YH, Gong M (2012) Measurement of wood shrinkage in jack pine using three dimensional digital image correlation (DIC). Holzforschung 66:639-643.

Silva C, Branco JM, Camoes A, Lourenco PB (2014) Dimensional variation of three softwood due to hygroscopic behavior. Constr Build Mater 59:25-31.

Stohr HP (1988) Shrinkage differential as a measure for drying stress determination. Wood Sci Technol 22:121-128.

USDA (2010) Wood handbook. General Technical Report GTR-190. U.S. Department of Agriculture, Forest Service, Madison, WI.

Welch MB (1932) The longitudinal variation of timber during seasoning. J Proc R Soc NSW 66:492-497.

Xavier J, De Jesus AMP, Morais JJL, Pinto JMT (2012) Stereovision measurements on evaluating the modulus of elasticity of wood by compression tests parallel to the grain. Constr Build Mater 26:207-215.

Yang TH, Wang SY, Tsai MJ, Lin CY (2009) The charring depth and charring rate of glued laminated timber after a standard fire exposure test. Build Environ 44:231-236.

Zhou HZ, Zhu EC, Fortino S, Toratti T (2010) Modelling the hygrothermal stress in curved glulam beams. J Strain Anal Eng Des 45:129-140.